



Qualitative risk assessment of soil erosion for karst landforms in Chahe town, Southwest China: A hazard index approach



Wei Huang^a, Hung Chak Ho^b, Yanya Peng^c, Lu Li^d

^a Department of Geography, School of Geographic and Environmental Science, Guizhou Normal University, No.116 BaoshanBeiLu, Guiyang 550001, Guizhou, China

^b Institute of Environment, Energy and Sustainability, The Chinese University of Hong Kong, Hong Kong

^c School of Arts, Guizhou Normal University, No.116 BaoshanBeiLu, Guiyang 550001, Guizhou, China

^d Faculty of Environmental Engineering, The University of Kitakyushu, Kitakyushu, Fukuoka 802-0841, Japan

ARTICLE INFO

Article history:

Received 14 June 2013

Received in revised form 22 April 2016

Accepted 9 May 2016

Keywords:

Chahe town

Guizhou

Karst

Soil erosion

Rocky desertification

GIS and remote sensing

Soil erosion hazard mapping

ABSTRACT

Accelerated soil erosion, rocky desertification and land degradation are three major threats to sustainable agricultural and regional development in karst landscapes, especially in developing countries. Soil erosion mapping is indispensable for monitoring such environmental changes. In Chahe town, Guizhou, southwest China, the karst area has suffered severe soil erosion in the second half of the twentieth century. In order to understand the erosion situation and conduct risk evaluation, erosion factors such as rainfall, vegetation cover, slope, land cover and soil type were integrated by combining spatial data of four different years and using GIS and remote sensing (RS) techniques to evaluate and map erosion risks. The soil erosion hazard analysis indicates that an average of 42% of the study area was covered by the moderate erosion throughout the study period. Understanding the spatial and temporal patterns of accelerated erosion helps to identify appropriate mitigation measures, and suggests that remediation of the karst landscape is progressing slowly, with considerable potential for further recovery.

© 2016 Elsevier B.V. All rights reserved.

1. Introduction

Anthropogenic soil erosion is a form of soil degradation that accelerates the geomorphic processes of natural soil erosion (Lal, 2001). Rocky desertification is a result of accelerated anthropogenic soil erosion. Rocky desertification can refer to the processes that collectively transform an area previously covered by vegetation and soil into a barren, rocky landscape (Yuan, 1997). According to Lal (2001), accelerated anthropogenic soil erosion and rock desertification are the major environmental problems in developing countries. Deforestation, overgrazing and unsuitable cultivation practices in developing countries accelerate the soil erosion rate, especially the rate of water induced soil erosion. Soil erosion becomes the most important land degradation problem worldwide (Eswaran et al., 2001) and creates a long-term negative impact on the soil properties (e.g. nutrient losses and reduction of water-holding capacities).

In Southeast Asia and the southwestern part of China, rock desertification is a serious issue accompanied with soil erosion in the karst areas. Socioeconomic factors such as poverty, irrational/intensive land use and local agriculture practice (Wang et al., 2004) increase the erosion rate, resulting in increased depletion of topsoil and exposure of rocky debris. This issue is a serious threat to the long-term sustainability of

agricultural productivity and regional development. In order to solve this problem, accurate soil erosion assessment is needed to qualify and quantify the risks of land degradation from land use change and regional development.

Traditional soil erosion assessment is limited by its data quality and model structure (Van Rompaey and Govers, 2002). It is ineffective to predict soil risks over a large spatial extent (e.g. regional scale). Increasing sophistication and cost-effectiveness of spatial technologies enhance soil erosion assessment, monitoring and control. In particular, remote sensing provides homogeneous data over large spatial extent with a revisit capability at multi-temporal scale (King and Delpont, 1993; Siakeu and Oguchi, 2000).

Previous GIS-based soil erosion assessments on karst landscapes were often done using quantitative models that calculated the volume of soil loss (Drzewiecki et al., 2013; Peng et al., 2008; Xu et al., 2008; Xu et al., 2009). The approach included the Universal Soil Loss Equation (USLE) (Wischmeier and Smith, 1978) and Revised Universal Soil Loss Equation (RUSLE) (Renard et al., 1997) to assess the land degradation. USLE and RUSLE are the models using lumped-parameter statistical methods for estimating net erosion on individual slopes. These models can generally evaluate the erosion risks in regional landscapes, but may not be practical in specific environment due to the lack of detailed data to fit the model parameters (Kheir et al., 2008). Some of the parameters of USLE and RUSLE are fixed data that highly depend on regional, spatial, and environmental contexts. These might be invalid in certain

E-mail address: weihuang@uwm.edu (W. Huang).

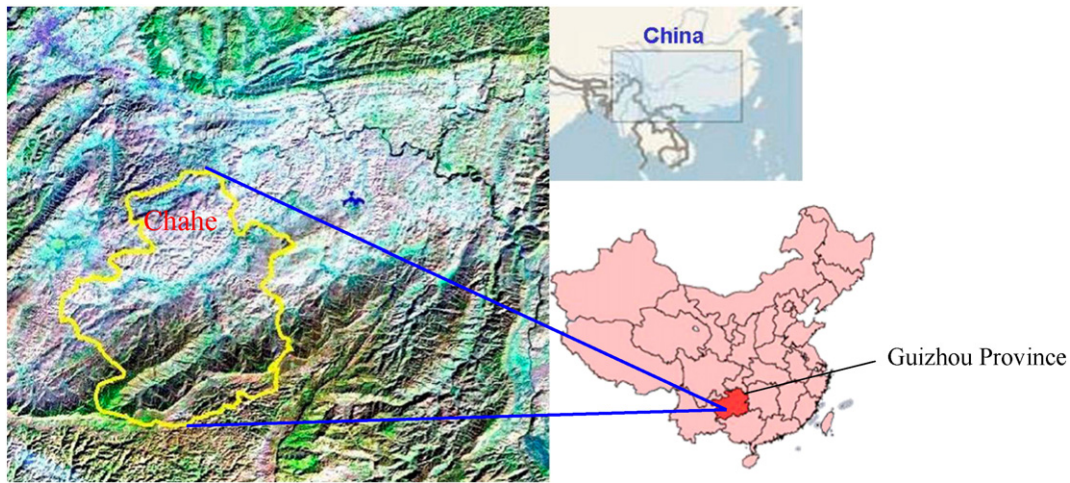


Fig. 1. Location of Chahe Town in Guizhou Province, China.

circumstances that local hydrological and agricultural data are not available (Warren, 2002).

Different from the quantitative approach, the qualitative method assigns weights to various spatial units to express intensity of the erosion. The qualitative model generally considered same erosion controlling factors as the quantitative models (e.g. slope, soil properties, vegetation cover and rainfall) but it assigned a specific weight to each erosion controlling factor based on the judgment or knowledge of local erosion processes from the researchers, and the importance of each factor in influencing the erosion process (Khan et al., 2001; Kheir et al., 2008; Vrieling, 2006). After the determination of weight, the value of all erosion factors are overlaid and multiplied with assigned weight to demonstrate the hazard condition (Rahman et al., 2009). This process is also known as the multi-criterion evaluation (MCE) approach, a fuzzy logic model that can be easily adapted to any environment and involves the determination of the spatial criteria, by assigning the weights and aggregating predefined rules to estimate the overall level of the hazard (Malczewski, 2004; Chen et al., 2010). The application of MCE has been extended to major research fields (e.g. geology, land use studies) in combining with geographic information system (GIS) in recent years (Beucher et al., 2014; Elaalem, 2013; Ho et al., 2014; Van Ranst et al., 1996), and has been successfully applied to classify the erosion intensity in a Mediterranean karst environment (Kheir et al., 2008). The

results from the previous studies such as Kheir et al. (2008) suggested that qualitative erosion assessment can be adapted to local setting and is able to assess soil erosion risks in karst environments. However, because of a particular social-economic and environmental settings (e.g. population density, social structure, governmental policy, type of agricultural practices, and karst landscapes) in the Southwest China karst environment, European-based soil model, such as Beucher et al. (2014) and Kheir et al. (2008) may not be the suitable approach to assess soil erosion risks in this study. Nevertheless, due to limited data availability, highly variable and complex erosion processes in different regional scale, most of current soil erosion studies in China are still in the primitive stage of erosion assessment (Peng et al., 2008). Specifically, in the remote rural karst areas of southwest China, the knowledge of local erosion processes is insufficient and the ancillary data are often unavailable. Therefore, it is recommend that qualitative method should be applied in the early stage of erosion assessment and quantitative method can be applied thereafter when abundant information of local erosion process has been collected (Vrieling, 2006).

The objective of this study is to 1) develop a GIS-based qualitative model based on local erosion processes to assess soil erosion risks of karst environments, 2) calculate a soil hazard index based on the qualitative model and 3) evaluate the distribution and intensity of local soil erosion. This study includes using GIS and remotely sensed data to



Fig. 2. (a) Rocky desertification in Chahe, (b) Northern Chahe, where severe erosion is now under control.

Table 1
Details of the satellite imagery used in the study.

Satellite sensor	Spatial resolution	Scene date	Original Projection System	Other details
Landsat TM	30 m	Sep 15, 1988	UTM	Orthorectified
Landsat TM	30 m	Dec 27, 1999	Space oblique Mercator B	Orthorectified
Landsat ETM +	30 m	May 14, 2002	UTM	Orthorectified
Aster VNIR	15 m	Feb 21, 2003	Geographic (Lat/Lon)	L1B product Orthorectified
SRTM	90 m	2001	Geographic (Lat/Lon)	

develop high quality dataset as the input data of the model. Relevant techniques are also employed to derive the parameters influencing the occurrence of erosion process over the study site.

2. Study area

Study site of this research is in Chahe Town, China. Situated in the southwestern suburb of Bijie City in Guizhou Province, it has a total area of 129.4 km². This area is covered with an extensive karst landscape and located at 27°05′–27°14′N and 105°17′–105°25′E (Fig. 1).

The climate of Chahe town is subtropical, with an average annual rainfall of 1150 mm and a mean annual temperature of 15 °C (Zhang, 1999). The area has a long history of agriculture, particularly growing tobacco and corn (Compilation Committee of Bijie Chronicles, 1994). Because of intensive agricultural practices and deforestation from the radical government campaign, severe soil erosion and rocky desertification occurred in Chahe Town for decades following deforestation beginning in 1958 (Liu and Huang, 2004). Excess amounts of steel production, and extensive areas of deforestation to provide fuel for furnaces and rapidly expanded agricultural programs caused massive soil disturbance. The nature of the karst landscape accentuated the erosion and makes it more difficult to control and recover from the accelerated erosion. As a result, deforestation dramatically accelerated soil erosion throughout the ensuing decades. Therefore, Bijie city ranked as the most severe soil erosion region in Guizhou Province (Zhang, 1999) and Chahe Town faced serious rocky desertification prevalent within the karst landscape (Fig. 2a).

Beginning in the 1980s, local government realized the seriousness of problem. It established an experimental area in 1988 (Zhang, 2013) and launched a campaign of planting trees and other plants suitable for this region, together with terracing and other soil conservation measures. With the purpose of recovering the vegetation and restoring the ecological system, the campaign has made considerable progress in parts of the region, although long-term and persistent efforts are still necessary

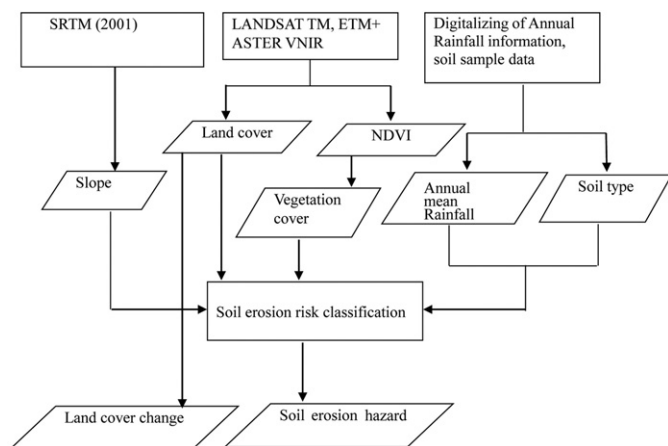


Fig. 3. Methodology of the study. SRTM data was converted to the slope map for terrain analysis. Satellite images was used to derive land cover and vegetation cover maps. Rainfall and soil type datasets were digitalized from the field data. The variables above were used in the spatial model to evaluate levels of local soil erosion hazard.

(Liu and Huang, 2004). Some measure of the current situation is depicted in Fig. 2b.

3. Material and method

3.1. Data sources and pre-processing of satellite imagery

Four satellite images, acquired from Sep 15, 1988; Dec 27, 1999; May 14, 2002 and Feb 21, 2003 respectively, were included in the study. The timeline of these images was corresponded with the winter and summer season. Landsat TM imageries of 1988 and 1999, and Landsat ETM + of 2002 were acquired from the Global Land Cover Facility from the University of Maryland (<http://glcf.umd.edu/>). ASTER Visible Near Infrared Bands (Band 1, 2, 3b and 3n) of 2003 was acquired from ASTER GDS web site (<http://gds.aster.ersdac.jspacesystems.or.jp>). Digital elevation model was derived from the SRTM (Shuttle Radar Topography Mission) (Reuter et al., 2007) data via the web site of USGS (<http://srtm.usgs.gov>). Details of the remotely sensed data are shown in Table 1.

Preprocessing work was conducted before the formal image processing. First, the projection of all images was converted to UTM and WGS84 datum with Zone 48N. Then the study area was subset from the original satellite imagery. The sensor calibration and atmospheric correction was also conducted to eliminate possible distortion or error of the imagery.

3.2. Post processing

The general procedure flow was as demonstrated in Fig. 3. There are several major steps in this approach.

First, slope information was extracted from DEM data. The DEM used in this study came from SRTM (Shuttle Radar Topography Mission) 2001 imagery generated by NASA and the National Imagery and Mapping Agency (NIMA). In this study, the SRTM 3 arc sec was used, having a horizontal grid spacing of 3 arc sec (approximately 90 m). Using ERDAS Imagine 9.1, the original DEM was processed and developed into slope map. All slopes were classified into 5 categories with the unit of angle degree: 0–8, 8–15, 15–25, 25–35, and 35–55.

Land cover is an indicator of land occupation, land use, soil utilization and resource distribution. It permits interpretation of the interactions of material and energy between human society and the natural environment. In this capacity, it is an important factor that influences the distribution and extent of soil erosion if it changes frequently within a short period of time. Land cover classification in this research was based on the field survey and supervised classification of the remote sensing images using ERDAS Imagine 9.1. All the images were divided

Table 2
Classification of vegetation coverage according to NDVI value.

Vegetation coverage	NDVI value
<10%	0.1029
10–30%	0.1029–0.3123
30–45%	0.3123–0.5513
45–60%	0.5513–0.7371
>60%	>0.7371

Table 3
Assigned value for soil erosion controlling factors.

Erosion factor					Assigned value
Annual rainfall (mm)	Vegetation Coverage (percentage)	Slope (angle gradient)	Land cover	Soil type	
<300	>60	0–8	Forest	Calcaric regosols	1
300–600	45–60	8–15	Shrub land	Haplic alisols	2
600–900	30–45	15–25	Farmland	Haplic luvisols, Chromic luvisols	3
900–1200	10–30	25–35	Bare land	Cumulic anthrosols	4
>1200	<10	35–55	Stony bare land	Dystric cambisols	5

into 5 land cover classes: forest, farm land, shrub land, bare land, and stony bare land (bare land with stony desertification). In the image of 2000, the class of river/pond was included because there was a storm event prior to the acquisition of satellite imagery (Wu, 2002) and the flooding zones on the satellite image for this year was very distinct and cannot be neglected.

The Normalized Difference Vegetation Index (NDVI) is one of the most widely used vegetation indices. NDVI is defined by the following equation (Tucker, 1979):

$$NDVI = \frac{NIR - RED}{NIR + RED} \quad (1)$$

NIR—Near infrared Band, RED—Red light wave Band.

For the Landsat Thematic Mapper (TM) sensor, Multi-spectral sensor and Enhanced Thematic Mapper Plus (ETM+) Multi-spectral sensor, the equation is:

$$NDVI = \frac{Band4 - Band3}{Band4 + Band3} \quad (2)$$

For the Aster Visible and Near-infrared Radiometer (VNIR), the equation is:

$$NDVI = \frac{Band3N - Band2}{Band3N + Band2} \quad (3)$$

Vegetation plays a fundamental role in controlling soil erosion, and vegetation coverage is frequently used as an indicator of extent and change in vegetation efficacy (Stow et al., 2004). In addition, soil loss tolerance varies considerably with different vegetation cover types (Zhang et al., 2003). Previous studies indicated that there is strong linear relationship between NDVI values and vegetation cover (Stow et al. 1993; Shippert et al. 1995). Therefore, NDVI has been used as a direct indicator of the protective vegetation cover (Gay et al., 2002; Jain and Goel, 2002; Cyr et al., 1995; Thiam, 2003). To derive the vegetation cover on the ground in the four scenes, NDVI values was first calculated. Then with the statistical function in ArcGIS 9.2, the NDVI values of vegetation were found to range from 0.1029 to 0.8 throughout the study area. Based on this, vegetation coverage was classified into five different categories, ranging from <10% to >60% (Table 2).

Table 4
Weight assignment based on Rank Sum Method.

Erosion factor (n = 5)	Straight rank (r _j)	Weight (n - r _j + 1)	Normalized weight	Weight (%)
Annual rainfall	1	5	0.33	33
Vegetation coverage	2	4	0.27	27
Slope	3	3	0.2	20
Land cover	4	2	0.13	13
Soil type	5	1	0.07	7
Sum		15	1	100

Annual rainfall data was based on the average rainfall between 1988 and 2003. The rainfall and soil type information were converted from local meteorological and geological reports into GIS shape file format, using digitization and related file manipulation in ArcGIS 9.2.

Evaluation of soil erosion hazard was based a multi-criteria decision process. UNEP (1997) defined a framework for mapping and measurement of rainfall-induced erosion in which soil type, land use, vegetation cover, and slope were integrated to generate an erosion risk map. Five erosion factors were used to determine and categorize soil erosion and each factor is also divided to five different levels with assigned values. The assigned value of the five factors was shown in Table 3, in which soil erosion risk is graded into five levels defined as not apparent, low, moderate, high and severe. The erosion risk of the study area is calculated by using the following equation:

$$E_i = \sum_{j=1}^n W_j * E_{ij} \quad (4)$$

where E_i is the erosion risk index of a place in the study area; W_j is the weight of factor j; E_{ij} is the erosion risk value under factor j and n is the total number of factors.

In order to determine the weight for each erosion controlling factor, the study used the rank sum method (Stillwell et al., 1981). The weights were calculated with the following equation:

$$w_j = \frac{n - r_j + 1}{\sum_{j=1}^n (n - r_j + 1)} \quad (5)$$

where w_j is the normalized weight of factor j; r_j is the rank position of factor j; $\sum_{j=1}^n (n - r_j + 1)$ is the total sum of all normalized weights and n is the total number of factors. The normalized weight is calculated from the ratio of individual weight to the sum of all weights. Erosion factors are ranked according to their relative importance of influencing local erosion occurrence. The calculated weights are displayed in Table 4.

After calculating the weight for each factor, the study converted each layer of the factors to raster format and used raster calculators to generate the value for erosion risk index with the following equation derived

Table 5
Land cover patterns and their correspondent area percentage.

Type	Year			
	1988	1999	2002	2003
Forest	5.27%	10.38%	9.75%	10.23%
Shrub land	30.47%	11.62%	10.19%	15.67%
Farm land	17.53%	20.95%	20.48%	23.95%
Bare land	23.46%	30.82%	31.59%	26.29%
Stony bare land	23.27%	26.23%	27.99%	23.86%

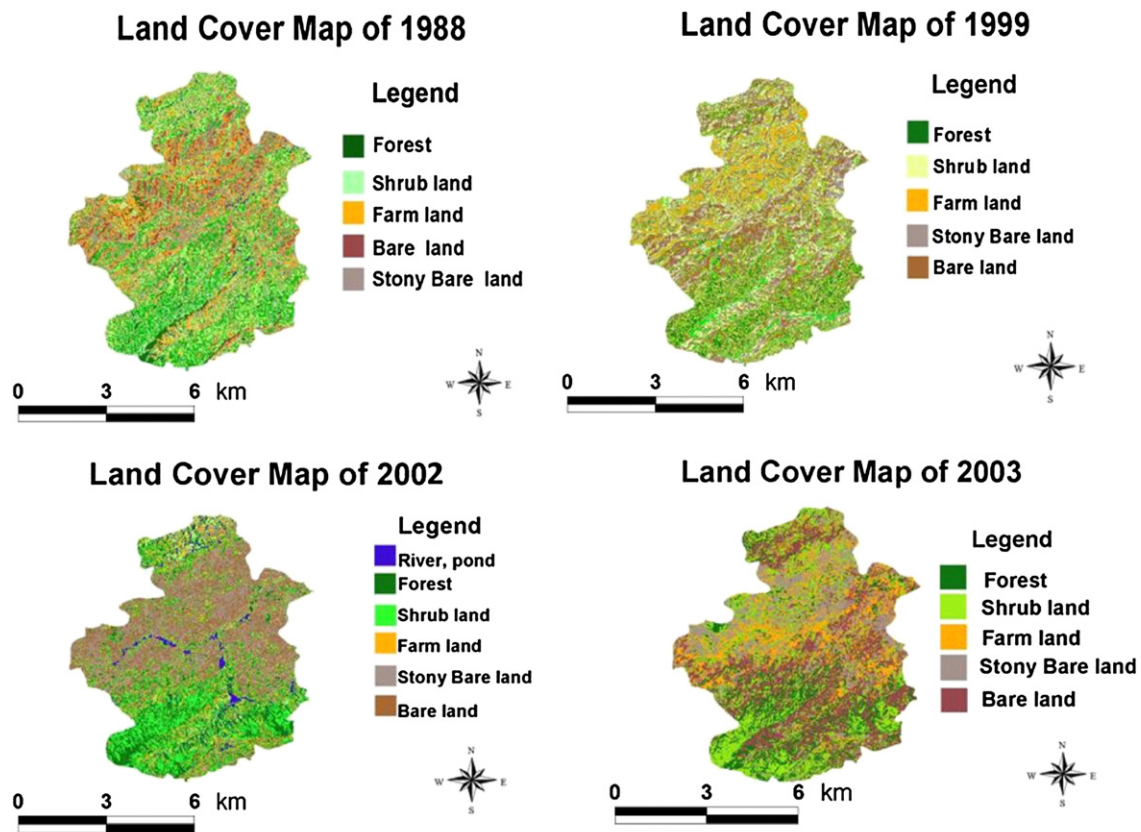


Fig. 4. Land cover map of 1988, 1999, 2002 and 2003. There are forest, shrub land, farm land, bare land and stony bare land in each map. The map of 2002 has one additional type of river and pond resulting from a storm event.

from Eq. (1) and Table 5:

$$\begin{aligned} \text{Erosion risk index} = & 0.33 * \text{rainfall} + 0.27 * \text{vegetation coverage} \\ & + 0.2 * \text{slope} + 0.13 * \text{landcover} + 0.07 \\ & * \text{soil type.} \end{aligned} \quad (6)$$

The overlay operation was completed in ArcGIS 9.2. Areas covered by flood in 2002 were excluded in the overlay process.

In order to validate the result of erosion risk analysis, a field survey was conducted on May of 2003, using a total of 215 sample points.

4. Result and discussion

4.1. Land cover and land cover change

The area percentage of each land cover category was derived from the land cover map (Fig. 4). The numeric results were compared in Table 5.

Table 5 shows a significant change of land cover over the year from 1988 to 2003. First, for forest, its area coverage increased from 5.27% in 1988 to 10.38% in 1999. After a slight decrease in 2002, it reached 10.23% in 2003. Second, shrub land reached its lowest levels in 2002 and showed steady recovery thereafter. Meanwhile, farm land also increased from 1988 to 1999 due to agricultural development. The comparison between the change of forest, shrub land and farm land indicate that recovering forest is far more difficult than other plants due to the thinness of top soil and loss of organic matter. Also, the shrub land is the only type that shows the rate of change >10% from 1988 to 2003. Bare land and the stony bare land occupied almost half of the land cover, they reached the highest levels in 2002, and have decreased thereafter.

4.2. Accuracy assessment of land cover classification

Accuracy assessment for the classification of land cover was conducted in ERDAS IMAGINE 9.1, using a total of 75 sample points in different land cover types across the study area. The overall accuracy for the four scenes was higher than 80% and the Kappa statistics showed a value higher than 0.7 (Table 6).

4.3. The relation between NDVI and vegetation cover

The vegetation cover map (Fig. 5) shows that the vegetation coverage percentage reached its lowest value in 1999, and increased from 2002 to 2003.

To evaluate the efficiency and accuracy of the division rule defined in Table 2, the correlation between the NDVI and vegetation coverage needs to be examined and assessed. Twenty sample points were used for the statistical analysis between previous surveys (Compilation Committee of Bijie Chronicles, 2005) and NDVI values. Each sample was retrieved from each sample site across the study area (Fig. 9). The result indicated that the vegetation coverage and NDVI had a high degree of positive correlation with over 0.7 of R square for all scenes (Fig. 6). Because the time of image acquisition corresponds with the winter and summer season and NDVI detects the vegetation vitality, the deciduous plants will not present their existence in winter season. On the other hand, both evergreen and deciduous plants can be detected on the satellite imagery in summer season. The general pattern of the chart showed that NDVI values appear higher than vegetation cover in summer than winter, and the overall area land cover also influence the NDVI value. In addition, the correlation chart for the September of 1988 also showed more outliers above the trend line than other years. Compared with Table 5, it also indicated that NDVI values appear higher

Table 6
Accuracy report for total land cover classification.

Class name	Reference totals	Classified total	Number correct	Producers accuracy	User accuracy
1988 (Kappa statistics = 0.71)					
Forest	5	5	5	100%	100%
Shrub land	20	25	20	100%	80%
Farm land	10	10	5	50%	50%
Bare land	10	10	10	100%	100%
Stony bare land	30	25	25	83%	100%
total	75	75	65		
Overall Classification Accuracy = 87%					
1999 (Kappa statistics = 0.75)					
Class name	Reference totals	Classified total	Number correct	Producers accuracy	User accuracy
Forest	20	30	20	100%	67%
Shrub land	10	10	10	100%	100%
Farm land	5	5	5	100%	100%
Bare land	15	10	10	67%	100%
Stony bare land	25	20	15	60%	75%
total	75	75	60		
Overall Classification Accuracy = 80%					
2002 (Kappa statistics = 0.72)					
Class name	Reference totals	Classified total	Number correct	Producers accuracy	User accuracy
River, pond	10	10	10	100%	100%
Forest	10	10	10	100%	100%
Shrub land	5	5	5	100%	100%
Farm land	10	10	5	50%	50%
Bare land	25	30	25	100%	83%
Stony bare land	15	10	10	67%	100%
total	75	75	65		
Overall Classification Accuracy = 87%					
2003 (Kappa statistics = 0.75)					
Class name	Reference totals	Classified total	Number correct	Producers accuracy	User accuracy
Forest	10	10	10	100%	100%
Shrub land	5	5	5	100%	100%
Farm land	10	10	5	50%	50%
Bare land	35	30	30	86%	100%
Stony bare land	15	20	15	100%	75%
total	75	75	65		
Overall Classification Accuracy = 87%					

than vegetation cover in that year, which is due to the pronounced response from both evergreen and deciduous plants in the summer season and the overall higher area percentage of all vegetation (forest, shrub land, and farm land together) than other years.

4.4. Slope, rainfall, and soil type

The slope map (Fig. 7a) showed that steep slopes, characteristic of mountainous areas are mainly concentrated in the southern section of Chahe town. The annual rainfall map (Fig. 7b) showed that the regions in the south and southeast receive more precipitation than the north. The soil type map (Fig. 7c) was based on the soil classification taxonomy in China (Shi et al., 2006) and converted to the World Reference Base

Table 7
Statistic correlation between NDVI and vegetation cover.

Statistics year	Pearson correlation	Sample number	Lower bound under 95% confident interval	Upper bound under 95% confident interval	Standard error
1988	0.8879	20	0.734	0.955	0.108
1999	0.9687	20	0.921	0.988	0.058
2002	0.9571	20	0.893	0.983	0.068
2003	0.9547	20	0.887	0.982	0.070

Table 8
Category of erosion hazard rank.

Erosion hazard rank	Calculated index
Not apparent	1
Low	1–2
Moderate	2–3
High	3–4
Severe	4–5

Table 9
Confusion matrix of soil erosion classification.

Classified survey	Not apparent	Low	Moderate	High	Severe	User's accuracy (%)
Not apparent	21	10	3	0	0	61.76
Low	5	77	10	0	0	83.70
Moderate	1	2	68	1	0	94.44
High	0	0	3	7	1	63.64
Severe	0	0	1	1	4	66.67
Producer's accuracy (%)	77.78	86.52	80	77.78	80	82.33

(WRB) soil classification (FAO, 1998). The result shows that haplic alisols have the highest area percentage of all soils in the study area, followed by haplic luvisols, dystric cambisols, chromic luvisols, cumulic anthrosols, and calcaric regosols, respectively.

4.5. Assessment of soil erosion risk

The erosion hazard index was calculated by using Eq. (6) and reclassified with the rule defined in Table 8. The result (Fig. 8) indicates that most high and severe erosion occurred in central and south of the study area. In addition, high and severe erosion have gradually decreased in the north and moved to the south. In order to validate the result of erosion risk analysis, a field survey was conducted on May of 2003, using a total of 215 sample points. The samples were collected from 20 locations across the study area (Fig. 9). In each site, 10 samples were collected in a radius of 30 m with the exception that 17 samples for location 10 and 18 samples for location 11, respectively. The result (Table 9) showed that, for low and moderate erosion, they occupy most of the study area and the user's and producer's accuracy level are over 80% and the overall accuracy reached 82.33%. The user's accuracy for the level of not apparent was relatively lower than other levels because there are considerable amounts of samples were misclassified as the level of low erosion, which is a typical error due to the fact that the presence of the two levels are sometimes difficult to differentiate from each other.

The area index of different erosion risk level was derived from the erosion hazard map. It was used to compare various risk categories in terms of the area coverage. The result (Table 10) revealed that low and moderate erosion risks characterize most of the study region and both displayed significant changes from 1999 to 2003. The moderate erosion appeared to be under control since 1999, although the steadily increasing low erosion risk warrants caution. Specifically, an average of 42% of the study area was covered by the moderate erosion throughout the study period. The high erosion sections remained under 10 km²

Table 10
Area index of different erosion levels from 1988 to 2003.

Area of year Erosion risk (km ²)	1988	1999	2002	2003
Not apparent	28.121	25.125	23.157	15.746
Low	47.583	36.453	43.731	53.459
Moderate	46.737	65.237	53.457	53.295
High	6.852	2.411	8.947	6.806
Severe	0.107	0.174	0.108	0.094

and decreased since 2002. The severe erosion ranked as the lowest percentage among all categories and remained relative stable. For areas with erosion that appeared to be not apparent, they demonstrated a steady decrease over the study period.

Kappa statistics = 0.65.

4.6. Source of error and uncertainty for the estimation

Possible errors in the estimation of soil erosion come primarily from land cover classification and vegetation cover derivation. For land cover, the methodology of classification was based on supervised classification. It categorizes the images with a pixel by pixel approach, in the way that training site was designated before every pixel is compared with its nearest neighbor to find the matched pixels. This approach assumes that pixels in the image are pure and only stand for specific land cover. However, the pixels in the image are often mixtures of different land cover. Therefore, result of land cover is influenced by the pixel by pixel approach.

For vegetation cover, the uncertainty comes primarily from the NDVI. The satellite imageries were acquired from Sep 15, 1988; Dec 27, 1999; May 14, 2002 and Feb 21, 2003, respectively. This time line corresponds with the winter and summer season. Since NDVI detects

the vegetation vitality, the deciduous plants will not present their existence in winter season. For this reason, the vegetation cover in winter season (1999 and 2003) was underestimated. This also explains why NDVI values appear higher than vegetation cover in summer than winter, and the overall area land cover also influence the NDVI value.

5. Conclusion and future prospects

Chahe Town suffered severe soil erosion and rocky desertification for decades following deforestation beginning in 1958. The exposure of bedrocks from thin soils, developed joints and fractures of the outcrops, and quick infiltration of surface flow due to lack of abundant vegetation characterize this area. These features of local landform accentuated the erosion and make it more difficult to control and recover from the accelerated erosion. Local people have been aware of the seriousness of this issue and the potential consequences if effective counter measures are not taken, and their endeavors merit technological support.

The application of remote sensing and GIS technology efficiently estimates risk level of soil erosion in the study area. The model provides justification that the areas of high and severe erosion in Chahe Town have remained relatively stable in the past 20 years, necessitating continuous control and mitigation efforts, but overall the situation has not worsened, and has improved locally. Thus, the soil map can use for future environmental monitoring, such as making plan for crop rotation and tree planting.

In this context, studies of the karst geomorphology and hydrology will be complemented by further analysis of satellite imagery using GIS techniques. For example, image fusion could assist in allowing advantageous combination of the merits of original images. The ASTER image has higher resolution, providing detailed local information, while the LANDSAT images cover a broader time frame over the past

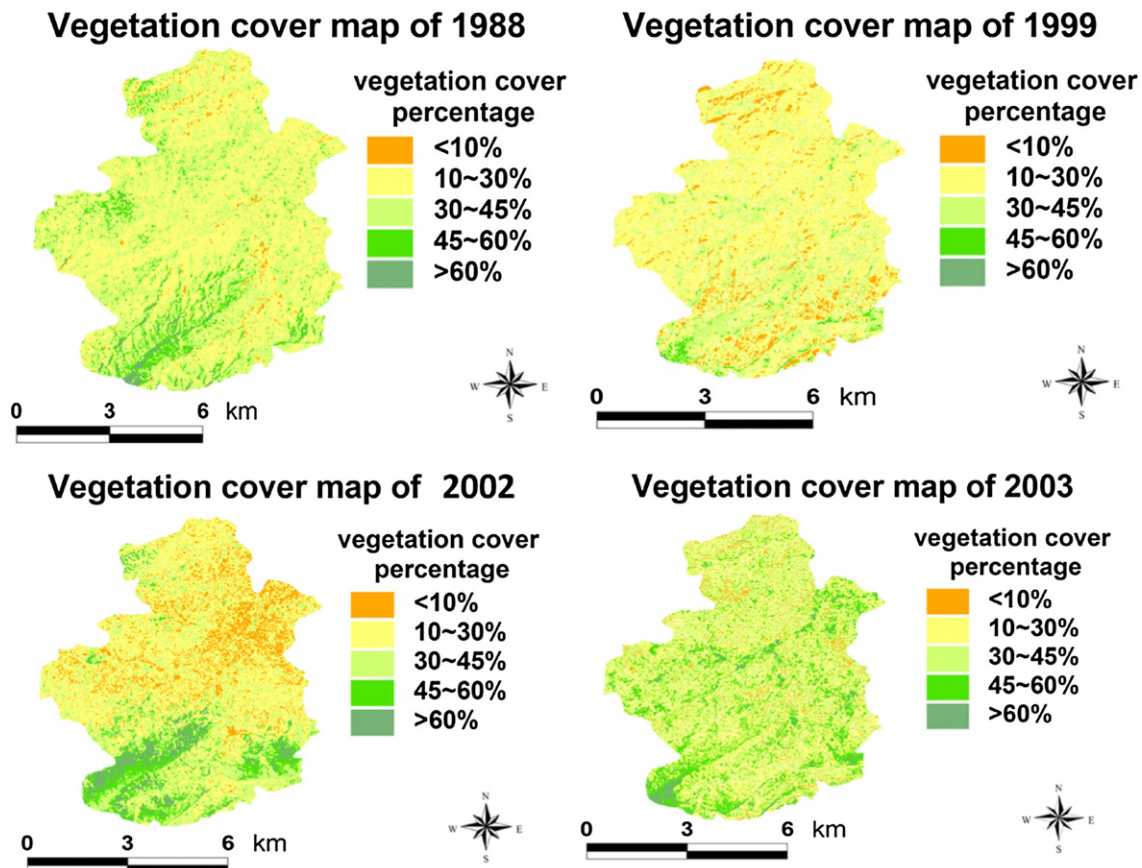


Fig. 5. Vegetation cover map of 1988, 1999, 2002 and 2003. The maps indicate that vegetation cover once decreased from 1988 to 2002, and proportionally increased thereafter.

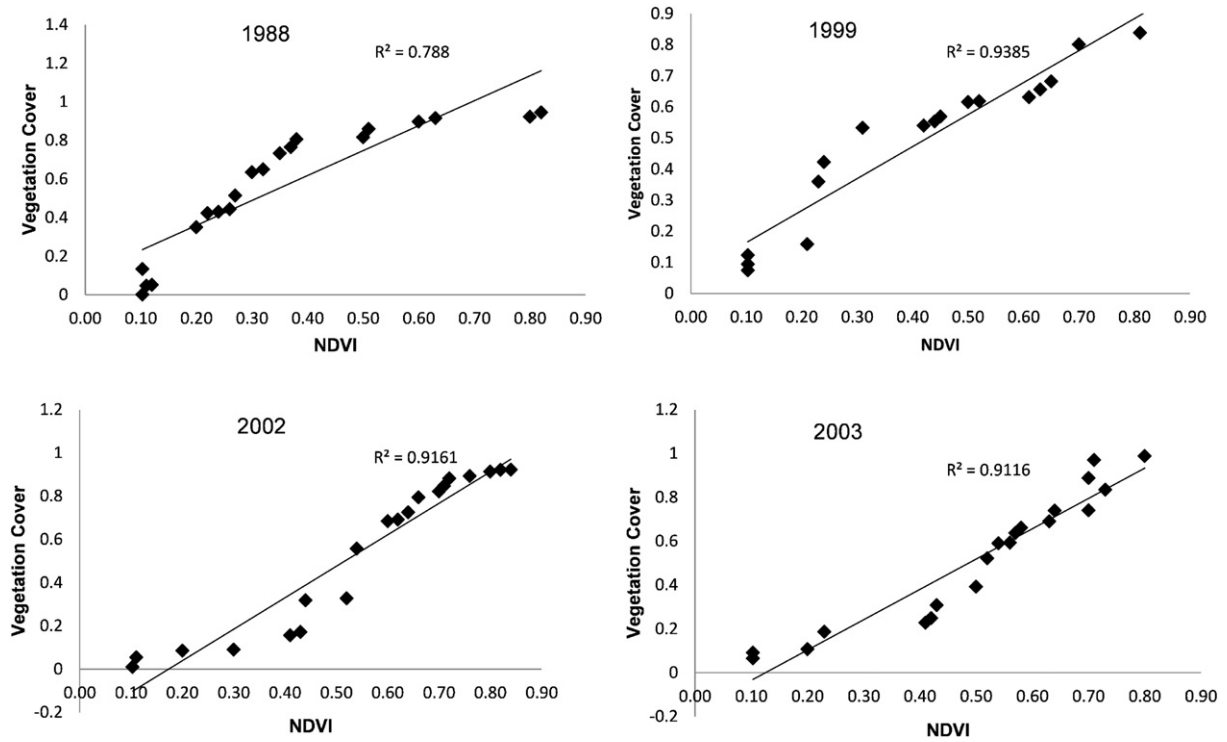


Fig. 6. Correlation between vegetation cover and NDVI, The charts indicate that overall correlation between NDVI and vegetation cover are higher than 0.7. Detailed statistics were described in Table 7. The table showed that NDVI and vegetation cover in 1999 have the highest Pearson correlation and the lowest stand standard error. The data in all other years have Person correlation higher than 0.8 and standard error lower than 0.2.

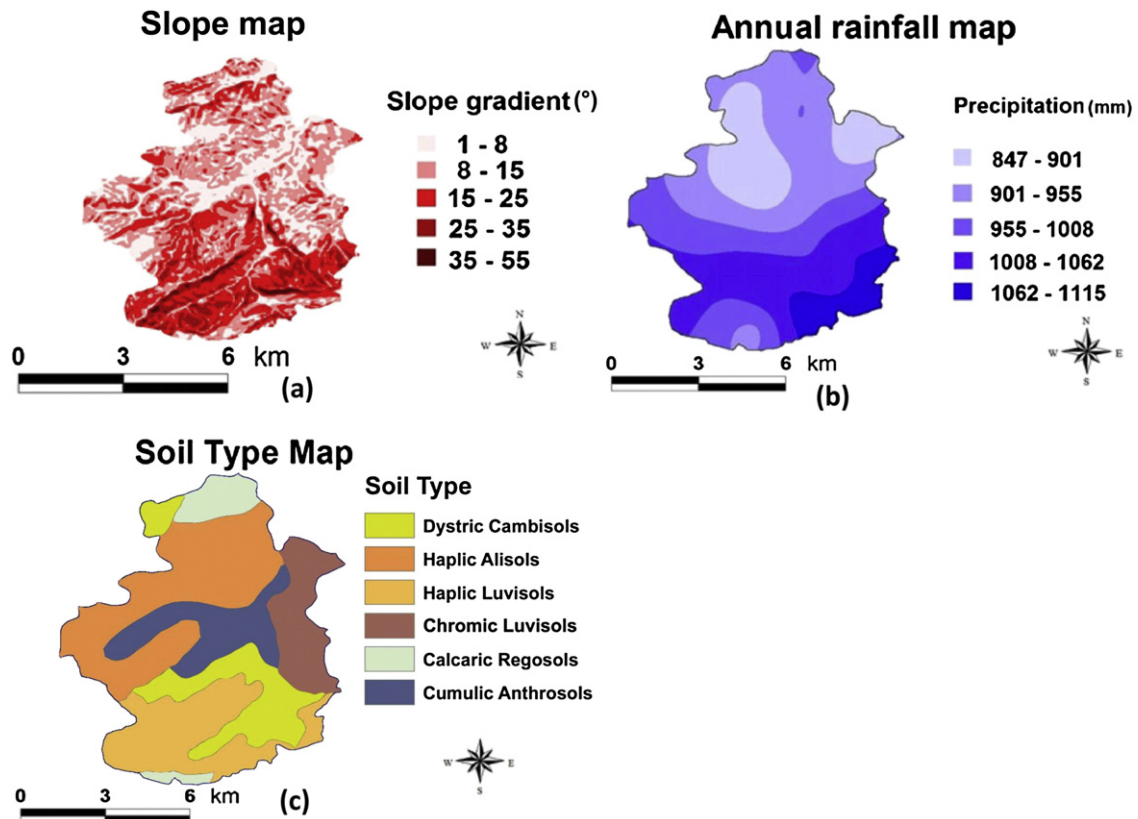


Fig. 7. (a) Slope map, (b) annual rainfall map, (c) soil type map. The maps show that southern part of the Chahe Town has steeper slope and higher annual rainfall.

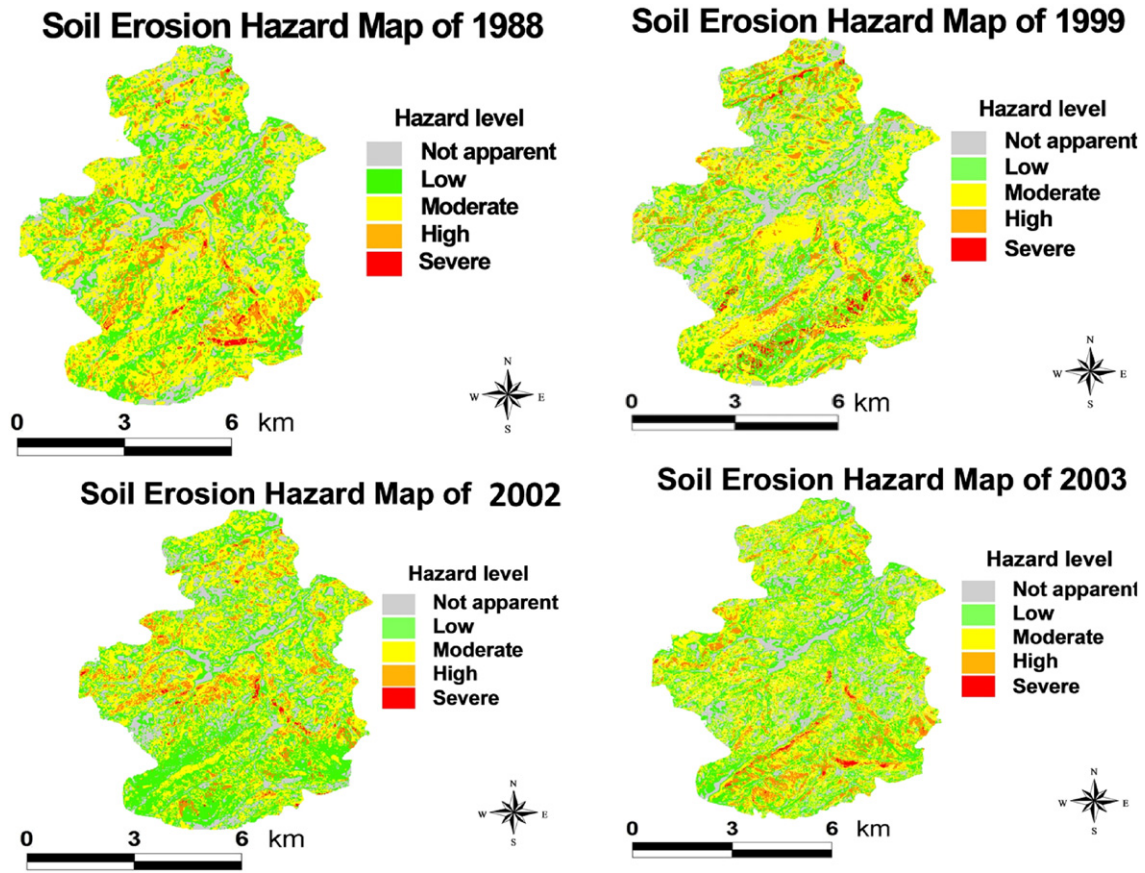


Fig. 8. Soil erosion hazard map of 1988, 1999, 2002 and 2003. Green indicates area in low risk from soil erosion, yellow area is the location with moderate soil erosion risk, orange indicates area with high soil erosion risks, and red is the locations with severe soil erosion risks.

20 years. In addition, hydrological analysis can also help to conduct a quantitative assessment when related local data becomes available in the future. Such technological applications can only contribute to the

resolution of soil erosion and rocky desertification in southwest China and elsewhere.

Acknowledgement

This paper was supported by the International Cooperation Grant QKHGW 2013-7043 from the Science and Technology Department of Guizhou Province, China. We would like to express our gratitude to Editor and two other reviewers for their helpful suggestions and valuable comments on earlier drafts of this manuscript.

Appendix A. Supplementary data

Supplementary data associated with this article can be found in the online version, at [doi:10.1016/j.catena.2016.05.008](https://doi.org/10.1016/j.catena.2016.05.008). These data include Google map of the most important areas described in this article.

References

- Beucher, A., Frojdo, S., Osterholm, P., Martinkauppi, A., Eden, P., 2014. Fuzzy logic for acid sulfate soil mapping: application to the southern part of the Finnish coastal areas. *Geoderma* 226–227, 21–30.
- Chen, Y., Yu, J., Khan, S., 2010. Spatial sensitivity analysis of multi-criteria weights in GIS-based land suitability evaluation. *Environ. Model. Softw.* 25 (12), 1582–1591.
- Compilation Committee of Bijie Chronicles, 1994. *Tobacco Chronicles of Bijie*. Guizhou People's Publishing House 389 pp.
- Compilation Committee of Bijie Chronicles, 2005. *Land Chronicles of Bijie*. Guizhou People's Publishing House 201 pp.
- Cyr, L., Bonn, F., Pesant, A., 1995. Vegetation indices derived from remote sensing for an estimation of soil protection against water erosion. *Ecol. Model.* 79, 277–285.
- Drzewiecki, W., Wezyk, P., Pierzchalski, M., Szafranska, B., 2013. Quantitative and Qualitative Assessment of Soil Erosion Risk in Małopolska (Poland), Supported by an Object-

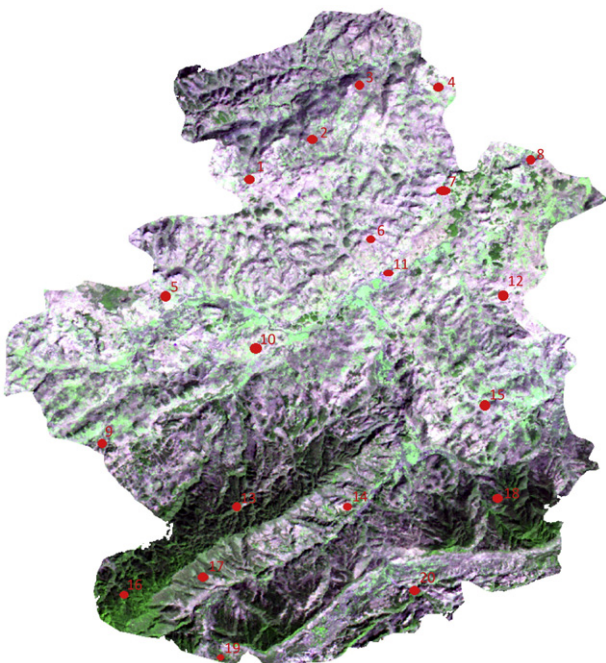


Fig. 9. Location of the sample sites for the soil erosion assessment.

- Based Analysis of High-Resolution Satellite Images. *Pure and Applied Geophysics* (In press).
- Elaalem, M., 2013. APCBEE Procedia 5, 405–409.
- Eswaran, H., Lal, R., Reich, P.F., 2001. Land degradation: an overview. In: Bridges, E.M., Hannam, I.D., Oldeman, L.R., Penning de Vries, F.W.T., Scherr, S.J., Sombatpanit, S. (Eds.), *Response to Land Degradation*. Science Publishers Inc., Enfield, NH, USA, pp. 20–35.
- Food and Agriculture Organization of the United Nations., 1998. *World Reference Base for Soil Resources*. Food and Agriculture Organization of the United Nations, Rome.
- Gay, M., Cheret, V., Denux, J.P., 2002. Apport de la télédétection dans l'identification du risque d'érosion. *La Houille Blanche* 2002 (1), 81–86.
- Ho, H.C., Mylorie, J.E., Infante, L.R., Rodgers III, J.C., 2014. Fuzzy-based spatial model approach to predict island karst distribution: a conceptual model. *Environ. Earth Sci.* 71, 1377–1396.
- Jain, S.K., Goel, M.K., 2002. Assessing the vulnerability to soil erosion of the Ukai Dam catchments using remote sensing and GIS. *Hydrol. Sci. J.* 47 (1), 31–40.
- Khan, M.A., Gupta, V.P., Moharana, P.C., 2001. Watershed prioritization using remote sensing and geographical information system: a case study from Guhiya, India. *J. Arid Environ.* 49 (3), 465–475.
- Kheir, R.B., Abdallah, C., Khawlie, M., 2008. Assessing soil erosion in Mediterranean karst landscapes of Lebanon using remote sensing and GIS. *Eng. Geol.* 99, 239–254.
- King, C., Delpont, G., 1993. Spatial assessment of erosion: contribution of remote sensing, a review. *Remote Sens. Rev.* 7, 223–232.
- Lal, R., 2001. Soil degradation by erosion. *Land Degrad. Dev.* 12 (6), 519–539.
- Liu, Z., Huang, Y., 2004. The fight for casting off the doom of being desert in Guizhou, Xinhua Net news. Retrieved from http://news.xinhuanet.com/focus/2004-06/07/content_1511535_1511535.htm.
- Malczewski, J., 2004. GIS-based land-use suitability analysis: a critical overview. *Prog. Plan.* 62 (1), 3–65.
- Peng, W.F., Zhou, J.M., He, Z.W., Yang, C.J., 2008. Integrated use of remote sensing and GIS for predicting soil erosion process. *Int. Arch. Photogramm. Remote. Sens. Spat. Inf. Sci. Vol. 37, 1647–1652 Part B4*. Beijing.
- Rahman, M.R., Shi, Z.H., Chongfa, C., 2009. Soil erosion hazard evaluation—an integrated use of remote sensing, GIS and statistical approaches with biophysical parameters towards management strategies. *Ecol. Model.* 220 (13), 1724–1734.
- Renard, K.G., Foster, G.R., Weesies, G.A., McCool, D.K., Yoder, D.C., 1997. Predicting soil erosion by water: a guide to conservation planning with the Revised Universal Soil Loss Equation. *Agricultural Handbook vol. 703* U.S. Department of Agriculture 404 pp.
- Reuter, H.I., Nelson, A., Jarvis, A., 2007. An evaluation of void-filling interpolation methods for SRTM data. *Int. J. Geogr. Inf. Sci.* 21 (9), 983–1008.
- Shi, X.Z., Yu, D.S., Warner, E.D., Sun, W.X., Petersen, G.W., Gong, Z.T., Lin, H., 2006. Cross-reference system for translating between genetic soil classification of China and soil taxonomy. *Soil Sci. Soc. Am. J.* 70, 78–83.
- Shippert, M.M., Walker, D.A., Auerbach, N.A., Lewis, B.E., 1995. Biomass and leaf-area index maps derived from SPOT images for Toolik Lake and Imnavait Creek areas, Alaska. *Polym. Recycl.* 31, 147–154.
- Siakeu, J., Oguchi, T., 2000. Soil erosion analysis and modelling: a review. *Trans. Jpn. Geomorphol.* 21 (4), 413–429.
- Stillwell, W.G., Seaver, D.A., Edwards, W., 1981. A comparison of weight approximation techniques in multiattribute utility decision making. *Organizational Behavior and Human Performance* 28, 62–77.
- Stow, D.A., Burns, B.H., Hope, A.S., 1993. Spectral, spatial and temporal characteristics of Arctic tundra reflectance. *Int. J. Remote Sens.* 14, 2445–2462.
- Stow, D.A., Hope, A., Mcguire, D., Verbyla, D., Gamon, J., Huemmrich, F., Houston, S., Racine, C., Sturm, M., Tape, K., Hinzman, L., Yoshikawa, K., Tweedie, C., Noyle, B., Silapaswan, C., Douglas, D., Griffith, B., Jia, G., Epstein, H., Walker, D., Daeschner, S., Petersen, A., Zhou, L., Myneni, R., 2004. Remote sensing of vegetation and land-cover change in Arctic tundra ecosystems. *Remote Sens. Environ.* 89, 281–308.
- Thiam, A.K., 2003. The causes and spatial pattern of land degradation risk in southern Mauritania using multitemporal AVHRR-NDVI imagery and field data. *Land Degrad. Dev.* 14 (1), 133–142.
- Tucker, C.J., 1979. Red and photographic infrared linear combinations for monitoring vegetation. *Remote Sens. Environ.* 8 (2), 127–150.
- UNEP, 1997. *Guidelines for Mapping and Measurement of Rainfall-Induced Erosion Processes in the Mediterranean Coastal Areas*, Priority Actions Program, Regional Activity Center. UNEP, Split.
- Van Ranst, E., Tang, H., Groenemam, R., Sinthurath, S., 1996. Application of fuzzy logic to land suitability for rubber production in peninsular Thailand. *Geoderma* 70 (1), 1–19.
- Van Rompaey, A.J.J., Govers, G., 2002. Data quality and model complexity for regional scale soil erosion prediction. *Geomorphology* 16 (7), 663–680.
- Vrieling, A., 2006. Satellite remote sensing for water erosion assessment: a review. *Catena* 65, 2–18.
- Wang, S.J., Liu, Q.M., Zhang, D.F., 2004. Karst rock desertification in Southwestern China: geomorphology, land use, impact and rehabilitation. *Land Degrad. Dev.* 15, 115–121.
- Warren, A., 2002. Land degradation is contextual. *Land Degrad. Dev.* 13 (6), 449–459.
- Wischmeier, W.H., Smith, D.D., 1978. Predicting rainfall-erosion losses: a guide to conservation planning. *Agricultural Handbook vol. 537* U.S. Department of Agriculture.
- Wu, H.Y., 2002. Meteorological analysis of May 13th storm event in Guizhou. *Meteorology of Guizhou* 26, 25–27.
- Xu, Y.Q., Shao, X.M., Kong, X.B., Peng, J., Cai, Y.L., 2008. Adapting the RUSLE and GIS to model soil erosion risk in a mountains karst watershed, Guizhou Province, China. *Environ. Monit. Assess.* 141 (1–3), 275–286.
- Xu, Y.Q., Peng, J., Shao, X.M., 2009. Assessment of soil erosion using RUSLE and GIS: a case study of the Maotiao River watershed, Guizhou Province, China. *Environ. Geol.* 56 (8), 1643–1652.
- Yuan, D., 1997. Rock desertification in the subtropical karst of south China. *Z. Geomorphol.* 108, 81–90.
- Zhang, J.P., 1999. Soil erosion in Guizhou province of China: a case study in Bijie prefecture. *Soil Use Manag.* 15, 68–70.
- Zhang, Y., Liu, B.Y., Zhang, Q.C., Xie, Y., 2003. Effect of different vegetation types on soil erosion by water. *J. Integr. Plant Biol.* 45, 1204–1209.
- Zhang, R., 2013. Current Situation, Problems and Countermeasures of Modern Agricultural Construction in Bijie Experimental Area. *Asian Agricultural Research* 5 (9), 25–28.